



#3799

Technical paper to be presented at the ASHRAE 1990 Winter Meeting, February 11-14, Atlanta Georgia. To be published in 1990 ASHRAE Transactions.

THEORETICAL AND COMPUTATIONAL INVESTIGATION OF SIMULTANEOUS HEAT AND MOISTURE TRANSFER IN BUILDINGS: "EVAPORATION AND CONDENSATION" THEORY

Alp Kerestecioglu (Member) Lixing Gu

ABSTRACT

Accurate modeling of combined heat and moisture transfer in buildings is important in predicting the indoor conditions, loads, comfort levels, degradation and deterioration of building components, and performance of mechanical equipment. This paper presents the "evaporation and condensation" theory, a set of spatially distributed equations for modeling detailed combined heat and moisture transport in building solids. The physical meaning of various transport coefficients and their influence on the overall transport phenomena are discussed. Associated material property requirements and data sources are also given.

The combined heat and moisture transfer equations for the building solids are solved by the finite element method. The finite element solutions are then interfaced with the exact solution of the air domain equations. Solutions from the equations are compared against analytical solutions of simplified cases. Simulation results are given to demonstrate the effectiveness of the theory.

Sample simulations showed that the amount of moisture adsorption or desorption by building materials to be significant. The temperature effects on moisture transfer found to be very important. Equations developed here found to predict the internal temperature and moisture (liquid and vapor) gradients satisfactorily, for limiting cases.

A. Kerestecioglu is a Research Associate; L. Gu, Graduate Research Assistant, Research and Development Division of the Florida Solar Energy Center, 300 State Road 401, Cape Canaveral, FL 32920.

INTRODUCTION

There are significant moisture problems associated with warm, humid climates. It is not uncommon in severely humid climates to have moisture loads in excess of 50 pounds per day (21.8 kg). In typical residences, these loads are removed by the air-conditioning system and do not generally cause serious problems. In passively cooled or energy-efficient buildings with standard air conditioners where sensible loads have been significantly reduced, these moisture loads may result in excessive relative humidity levels, even in air-conditioned buildings.

Methods of accurately evaluating moisture effects in buildings are generally lacking in building energy analysis procedures. Typically, simple procedures call for the calculation of sensible loads and the subsequent application of some percentage of that load to represent the additional moisture load of the conditioned space (zone). Where moisture loads are calculated by detailed procedures, the assumption is usually made that all moisture entering the zone is added to the zone air and none is adsorbed by the building materials. This assumption can produce inaccuracies. In reality, the moisture that is added to a conditioned zone will be distributed in some manner between the zone air, the zone materials, and the zone mechanical system.

In building simulations the researchers must be able to predict the indoor conditions and the associated loads. To accurately predict these variables, the transport equations must be solved for each building component. The solution to combined heat and moisture transfer equations in building solids can give the amount of moisture adsorption and desorption rates by building materials. If the equations for the building solids are simultaneously solved with zone energy and moisture balance equations, the effect of moisture adsorption and desorption of building materials on indoor conditions and associated loads can

be predicted.

This study presents the "evaporation and condensation" theory, a set of spatially distributed equations for modeling combined heat and moisture transport in building solids using the available material property data from the literature. As shown in Figure 1, for mathematical convenience, the building is divided into three domains: air (Ω_a), envelope (Ω_e) and furniture (Ω_f) and three surfaces: exterior envelope (Γ_e), interior envelope (Γ_a) and furniture (Γ_f). Moisture transport occurs in both the solid (Ω_e, Ω_f) and air (Ω_a) domains. In the air domain moisture exists as a vapor. However, in the solid domains moisture may occur in one or all of its three phases. In this study the combined heat and moisture transfer taking place in the envelope and furniture is formulated using spatially distributed equations, but the energy and moisture balance of the air domain are formulated using spatially lumped equations. The spatially lumped and distributed equations are interfaced at the domain boundaries (surfaces). A detailed derivation of a spatially lumped moisture model, called the "effective moisture penetration depth" model, and a literature survey of lumped models are given by Kerestecioglu et al. (1988.a).

Combined heat and moisture transport in materials is very difficult to describe mathematically. In addition to liquid molecular diffusion, transport by vapor diffusion, surface diffusion, Knudsen diffusion, capillary flow, purely hydrodynamic flow, and internal evaporation and condensation further complicate the problem. The traditional approach has been to sum the various contributions to the total flow of water (Luikov 1966; Philip and DeVries 1957; DeVries 1958 and 1987). This results in apparent (effective) water-diffusion and thermal-diffusion coefficients which relate the total water flux to the moisture and

temperature gradients. It should be noted that the temperature gradient is not related to the Soret effect, but is strictly dependent on the sorption isotherm, the evaporation and condensation mechanism of transport, and the temperature dependence of the capillary suction pressure (see Philip and DeVries 1957). Special mention must be made of the work of Harmathy (1969), who devised a theory for water transport in porous bodies assuming that all movement of water takes place in the vapor phase, but with porous structure permeability that is dependent on the moisture content. Special mention must be made also of Berger and Pei (1973), who account for vapor and liquid transfer using constant permeabilities.

During the 1960s it became fashionable to use flux equations that were based on the phenomenological theory of irreversible thermodynamics as developed by Prigogine (1961); Groot (1951 and 1961); Groot and Mazur (1962); and Fitts (1962). Examples of such studies are those of Luikov (1964, 1966 and 1975); soil-science applications by Cary and Taylor (1962); and studies of Taylor and Carey (1964); Roques and Cornish (1980); Valchar (1966) and, recently, Fortes and Okos (1978 and 1980). Most notably Luikov et al. (1964, 1966 and 1975) pursued this direction.

MATHEMATICAL FORMULATIONS

If the air is assumed to be well mixed, a set of ordinary differential equations can be written to represent the energy and moisture balances for the air domain ("zone" or room). The energy and moisture balance equations for a single "zone" can be written as the following equations:

$$\rho_a V C_p \frac{dT_r}{dt} = Q_T + m \cdot C_p (T_\alpha - T_r) + Q_{T,W} \text{ in } \Omega_a \quad (1)$$

$$\rho_a V \frac{dW_r}{dt} = Q_M + m \cdot (W_\alpha - W_r) + Q_{M,W} \text{ in } \Omega_a \quad (2)$$

with

$$\text{@ } t = 0 \quad T_r = T_{r,0} \quad \text{and} \quad W_r = W_{r,0}$$

The components of the energy and moisture balance equations and the parameters used in Eqs. (1) and (2) are illustrated in Figure 1. In Eqs. (1) and (2) Q_T and Q_M denote the thermal energy and moisture generations, respectively. The second term on the right-hand side of each equation denotes the infiltration load, and the last term in each equation denotes the thermal energy and moisture taken or released by the solid domains. They are defined by the following equations:

$$Q_{T,W} = \sum_{i=1}^{nos} A_i h_{T,i} (T_i^* - T_r) \text{ on } \Gamma_a \text{ and } \Gamma_f \quad (3)$$

and

$$Q_{M,W} = \sum_{i=1}^{nos} A_i h_{M,i}^* (W_i^* - W_r) \text{ on } \Gamma_a \text{ and } \Gamma_f \quad (4)$$

Equations (3) and (4) are important because they interface the air and solid domains. T^* and W^* denote the temperature and the humidity ratio of the surface, respectively. h_T and h_M^* are the convective heat and mass transfer coefficients, respectively, and A denotes the surface area. A detailed discussion of these terms is given in the succeeding sections. Equations (1) and (2) are not complete and, for simplicity, several terms are ignored. The complete equations are given by Kerestecioglu et al. (1988.a).

In the development of the combined heat and mass transfer equations for the solid domains the following assumptions are made: moisture travels due to water vapor density (partial water vapor pressure) gradients, local thermodynamic equilibrium exist, the total pressure is constant, and the solid matrix is rigid. With these assumptions the governing moisture and heat balance equations can be written as the following equations:

$$\Lambda \frac{\partial \rho_v}{\partial \tau} = \nabla \cdot (\Lambda D_v \nabla \rho_v) - \rho_b \frac{\partial U_e}{\partial \tau} \text{ in } \Omega_e \text{ and } \Omega_f \quad (5)$$

$$(\rho C_p)_e \frac{\partial T}{\partial \tau} = \nabla \cdot (k_e \nabla T) + \lambda \rho_b \frac{\partial U_e}{\partial \tau} \text{ in } \Omega_e \text{ and } \Omega_f \quad (6)$$

Equations (5) and (6) are the modified forms of the equations given by Crank (1964, pp. 307-308), and are referred to as "evaporation condensation" equations. Equation (5) states that the net amount of water vapor increase in the pores is equal to the amount of water vapor brought to the pore by diffusion minus the amount of liquid water accumulated. Similarly, Eq. (6) states that the net amount of energy stored in a control volume is equal to the amount of heat conducted plus the energy liberated during the phase conversion. Because local thermodynamic equilibrium is assumed to hold, the amount of liquid water at any given point can be calculated through the equilibrium sorption isotherm with the knowledge of the temperature and water vapor density at that point. The boundary conditions for these equations are given in the following equations:

$$-\Delta D_v \nabla \rho_v = \begin{cases} h_M (\rho_v^* - \rho_{v,\alpha}) & \text{on } \Gamma_e \\ h_M (\rho_v^* - \rho_T) & \text{on } \Gamma_a \text{ and } \Gamma_f \end{cases} \quad (7)$$

and

$$-k_e \nabla T = \begin{cases} -q''_T + h_T (T^* - T_\alpha) + \epsilon \sigma (T^{*4} - T_s^4) & \text{on } \Gamma_e \\ -q''_T + h_T (T^* - T_T) + \sum_{j=1}^{nos} \sigma F_{i-j} (T^{*4} - T_j^4) & \text{on } \Gamma_a \text{ and } \Gamma_f \end{cases} \quad (8)$$

Equations (7) and (8) are written in general and include all types of boundary conditions that might be encountered in buildings. Each equation consists of several terms that may be applicable either to the interior (solid to "zone") or exterior (solid to ambient) boundaries of the solid domain. Equation (7) can be obtained by writing a moisture balance at the boundaries of the solid domain. Equation (7) states that the amount of moisture diffusing is equal to convective moisture fluxes. Equation (8) can be obtained by writing an energy balance at the surface of the solid domain. Equation (8) states that the amount of heat conducted is equal to the summation of four components: imposed heat fluxes (such

as solar radiation), convective fluxes, radiation to a known source or sink (such as night sky radiation), and radiation among surfaces that view each other. In Equation (8) F_{i-j} denotes the script-F factor, which is a function of the view factors and the emissivity of the material (the mathematical derivation of the script-F factors is given in Kerestecioglu et al. (1988.b)).

In Eqs. (5) and (7) D_v denotes the vapor diffusivity of the material and can be related to the molecular diffusivity of water vapor in air, D_a , by the following equation (Philip and DeVries 1957; Luikov 1966; Fortes and Okos 1978; Pierce and Benner 1986).

$$D_v = (D_a/\tau_0) P/(P-P_v) \quad (9)$$

According to Sherwood and Pigford (1952), the molecular diffusivity of water vapor in air is given by the following equation (valid up to 1366 K)

$$D_a = (9.26 \times 10^{-4}/P) T^{2.5}/(T+245)$$

In Eq. (6) $(\rho C_p)_e$ and k_e denote the effective thermal capacity and the effective thermal conductivity of the material, respectively. If the porosity, Λ , is known, the effective thermal capacity and the effective thermal conductivity may be approximated according to the following equations:

$$(\rho C_p)_e = \Lambda (\rho C_p)_{air} + (1-\Lambda) (\rho C_p)_s \quad (10)$$

$$k_e = \Lambda k_{air} + (1-\Lambda) k_s \quad (11)$$

The equilibrium moisture content, U_e , used in Eqs. (5) and (6) is defined by the following equation (Kerestecioglu et al. 1988.b, Appendix D):

$$U_e = a \phi^b + c \phi^d \quad (12)$$

In Eq. (12) a, b, c and d are material-dependent constants. ϕ denotes the water activity (relative humidity in decimal form) and is defined by the following equations:

$$\phi = \rho_v/\rho_{v,sat} \quad (13)$$

and

$$\rho_{v, \text{sat}} = 1/(R_v T) \exp[23.7093 - 4111/(T-35.45)] \quad (14)$$

It should be noted that different forms of Eq. (12) are available and can be used. However, in this paper Eq. (12) is used to represent the sorption isotherm. World wide sorption isotherm data for various building materials are compiled and reduced to the format given by Eq. (12). (The data can be found in Kerestecioglu et al. (1988.b).

If Eqs. (13) and (14) are substituted into Eq. (12), and the result is differentiated with respect to time, τ , the following equation can be derived:

$$\frac{\partial U_e}{\partial \tau} = \frac{\partial U_e}{\partial \rho_v} \frac{\partial \rho_v}{\partial \tau} + \frac{\partial U_e}{\partial T} \frac{\partial T}{\partial \tau} = A_T \frac{\partial \rho_v}{\partial \tau} - B_\rho \frac{\partial T}{\partial \tau} \quad (15)$$

In Eq. (15) A_T and B_ρ denote the isothermal moisture capacity and the thermo-gradient coefficient of the material, respectively. Their magnitudes are defined by the following equations:

$$A_T = 1/\rho_v (ab \phi^b + cd \phi^d) \quad (16)$$

and

$$B_\rho = - [1/T - 4111/(T-35.45)^2] (ab \phi^b + cd \phi^d) \quad (17)$$

If a different form of Eq. (12) is used, Eqs. (16) and (17) must be rederived. The isothermal moisture capacity is analogous to the specific heat in heat transfer and indicates the relative moisture capacity of a material. The isothermal moisture capacity increases with increasing relative humidity and decreasing water vapor density. The thermo-gradient coefficient represents the effect of thermal gradients on moisture gradients within the material. This property increases with increasing relative humidity and decreasing temperature. If the thermo-gradient coefficient is small, the moisture transfer will not be influenced by thermal fields. Note that A_T and B_ρ are determined directly from the sorption isotherm. After substituting Eq. (15) into Eqs. (5) and (6), and eliminating U_e , the following set of equations can be obtained.

$$F_{11} \partial \rho_v / \partial \tau = \nabla \cdot (\Delta D_v \nabla \rho_v) + F_{12} \nabla \cdot (k_e \nabla T) \text{ in } \Omega_e \text{ and } \Omega_f \quad (18)$$

$$F_{21} \partial T / \partial \tau = \nabla \cdot (k_e \nabla T) + F_{22} \nabla \cdot (\Delta D_v \nabla \rho_v) \text{ in } \Omega_e \text{ and } \Omega_f \quad (19)$$

The coefficients F_{11} , F_{12} , F_{21} and F_{22} are defined according to the following equations:

$$F_{11} = \Lambda + \rho_b A_T - (\rho_b B_\rho \lambda \rho_b A_T) / [(\rho C_p)_e + \lambda \rho_b B_\rho] \quad F_{12} = (\rho_b B_\rho) / [(\rho C_p)_e + \lambda \rho_b B_\rho]$$

$$F_{21} = (\rho C_p)_e + \lambda \rho_b B_\rho - (\lambda \rho_b A_T \rho_b B_\rho) / (\Lambda + \rho_b A_T) \quad F_{22} = (\lambda \rho_b A_T) / (\Lambda + \rho_b A_T)$$

If Eqs. (18) and (19) are similar to the equations suggested by Luikov (1975); Philip and DeVries (1957) and many others. However, the cross terms used in these equations (the Laplacian of temperature in the mass transfer equation and the Laplacian of water vapor density in the heat transfer equation) are directly related to the sorption isotherm.

In Eqs. (10) and (11) the effective thermal capacity and the effective thermal conductivity of the material are defined as a linear fraction (determined by the porosity, Λ) of the moist air and the solid. An alternate form of estimating these effective properties is given below. In the following formulations the porosity is assumed to decrease with increasing moisture content, and the concept of static and dynamic porosities is introduced.

The volume of the solid, V_s , can be estimated if the total volume, V_t , and the static porosity, Λ_s , (measured when the material is completely dry) are known.

$$V_s = V_t (1 - \Lambda_s)$$

If the moisture content of the material, U , is known, the liquid volume, V_l , can be calculated with the following equation:

$$V_l = U \rho_s V_t / \rho_w$$

In the above equation, the moisture content, U , and the density of water, ρ_w , will spatially vary. Consequently, this equation should be integrated over the

total volume. Later the result should be divided by the total volume. The volume of the air and water vapor mixture, V_g , can be estimated with the following relation:

$$V_g = V_t - V_s - V_l$$

Consequently, the dynamic porosity, Λ_d , can be defined by the following equation:

$$\Lambda_d = V_g/V_t = 1 - (V_s+V_l)/V_t$$

With known volumes and primary physical properties the effective density, specific heat and thermal conductivity can be estimated through the following equations:

$$\rho_e = \frac{\sum_{i=1}^3 V_i \rho_i}{\sum_{i=1}^3 V_i} \quad C_{p,e} = \frac{\sum_{i=1}^3 V_i \rho_i C_{p,i}}{\sum_{i=1}^3 V_i \rho_i} \quad k_e = \frac{\sum_{i=1}^3 V_i k_i}{\sum_{i=1}^3 V_i}$$

$i=1$ represents the solid, $i=2$ represents the liquid water, and $i=3$ represents the air and water vapor mixture.

TECHNICAL NOTE ON DIFFUSIVITIES:

The vapor flux, J_v , based on water vapor density, ρ_v , is represented by the following equation:

$$J_v = - D_v \nabla \rho_v \quad (20)$$

however, if the ideal gas law is assumed to prevail, the vapor flux can also be written in terms of partial water vapor pressure, P_v , as the following equation:

$$J_v = - D_v/R_v T \nabla P_v \quad (21)$$

The water vapor diffusivity, D_v , used in Eqs. (20) and (21) is related to the molecular diffusivity of water vapor in air, D_a , through Eq. (9). From Equation (21) the permeability, π , of the material can be defined as the following equation:

$$\pi = D_v/R_v T \quad (22)$$

Using Eqs. (9) and (22) the tortuosity factor can be related to the permeability

by the following equation:

$$\tau_0 = D_a / (\pi R_v T) P / (P - P_v) \quad (23)$$

Sometimes rather than the permeability, the permeance, π_m , of the material is given. However, the permeability and the permeance of the material have the following relationship:

$$\pi_m = \pi / L \quad (24)$$

In Eq. (24), L denotes the length of the specimen where the permeance measurement was made. Before concluding the mathematical formulations a very important point must be clarified. Equations (5), (18) and (19) indicate that the only diffusivity required is the water vapor diffusivity. However, water can migrate in either vapor or liquid phases and most commonly moves in both phases. A common practice might be to write separate equations for the liquid and vapor fluxes. Later, via the local thermodynamic equilibrium assumption and Kelvin's equation, either the liquid flux can be related to the vapor flux or vice versa. If this procedure is followed, an effective diffusivity must be introduced. Luikov's (1975); Philip and DeVries's (1957); Berger and Pei's (1973) studies are some examples.

Consequently, the water vapor diffusivity defined by Eq. (9) must be viewed in the following manner. The tortuosity factor, τ_0 , may not be the true tortuosity, but is a factor that indicates the water vapor resistance of the material and is a function of the moisture content. For instance, Tveit's (1966) data indicates three conditions: with increasing moisture contents for most of the building materials the water vapor diffusivity increases; for some materials the water vapor diffusivity stays almost constant; and for some materials after an increase there is a noticeable decrease. These conditions can be attributed to liquid water movement and saturation of the pores. Saturation of the pores can

be handled through the static and dynamic porosity concept. Hence, if similar experiments are performed at a constant temperature as Tveit's experiments were performed, the tortuosity factor as a function of moisture content can be obtained. Similarly, if permeability measurements are performed, a difference among the dry- and wet-cup experiments is realized. Therefore, if Eq. (22) is used to obtain the water vapor diffusivity, permeability data at different moisture contents are necessary.

NUMERICAL SOLUTIONS

In the numerical solutions the two domains must be simultaneously considered. The "zone" energy and moisture balance equations, Eqs. (1) and (2), can be rearranged according to the following equations:

$$dT_r/dr + P_1(\tau) T_r = Q_1(\tau) \text{ in } \Omega_a \quad (25)$$

$$dW_r/dr + P_2(\tau) W_r = Q_2(\tau) \text{ in } \Omega_a \quad (26)$$

P_1 , P_2 , Q_1 and Q_2 are time dependent parameters and are defined by Kerestecioglu et al. (1989.a). The exact solutions of Eqs. (25) and (26) subject to initial conditions, are given as the following equations:

$$T_r(\tau) = Q_1(\tau)/P_1(\tau) + [T_{r,o} - Q_1(\tau)/P_1(\tau)] \exp[-P_1(\tau)\tau] \quad (27)$$

$$W_r(\tau) = Q_2(\tau)/P_2(\tau) + [W_{r,o} - Q_2(\tau)/P_2(\tau)] \exp[-P_2(\tau)\tau] \quad (28)$$

For the solution of the solid domains the Galerkin Finite Element Method (GFEM) is used. Eqs. (18) and (19) are multiplied by a weighing function and the residual is set to zero. Later, applying the Green-Gauss theorem on the second order terms, the boundary conditions given by Eqs. (7) and (8) are introduced. Equations (7) and (8) are boundary conditions to Eqs. (5) and (6) not to Eqs. (18) and (19). Therefore, modified boundary conditions must be used that would account for simultaneous temperature and vapor density gradients for each equation. The variation of the temperature and the water vapor density

throughout the solid domain is approximated in terms of nodal values a_T and a_ρ according to the following equations:

$$T = N a_T \quad \text{and} \quad \rho_v = N a_\rho$$

where N is the usual shape function defined for each element. For the standard GFEM the weighing functions are the shape functions. The algebraic GFEM formulations of the solid domains are given by the following equations:

$$C_T a_T + K_T a_T + K_{TM} a_\rho = F_T \quad (29)$$

$$C_M a_\rho + K_M a_\rho + K_{MT} a_T = F_M \quad (30)$$

The capacitance (C), stiffness (K) matrices and the force (F) vectors used in Eqs. (29) and (30) are given as the following equations:

$$C_T = \int_{\Omega} N^T \{F_{21}\} N \, d\Omega$$

$$K_T = \int_{\Omega} \frac{\partial N^T}{\partial x_k} \{k_e\} \frac{\partial N}{\partial x_k} \, d\Omega + \int_{\Gamma} N^T \{h_T\} N \, d\Gamma + \int_{\Gamma} N^T (Na_T)^3 \left\{ \sigma \left(\epsilon + \sum_{j=1}^{nos} F_{i-j} \right) \right\} N \, d\Gamma$$

$$K_{TM} = \int_{\Omega} \frac{\partial N^T}{\partial x_k} \{F_{22} \Delta D_v\} \frac{\partial N}{\partial x_k} \, d\Omega + \int_{\Gamma} N^T \{F_{22} h_M\} N \, d\Gamma$$

$$F_T = \int_{\Gamma} N^T \left\{ h_T T + \sigma \epsilon T s^4 + q''_T + \sum_{j=1}^{nos} \sigma F_{i-j} T_j^4 + F_{22} (h_M \rho_{v,\alpha} + q''_M) \right\} d\Gamma$$

$$C_M = \int_{\Omega} N^T \{F_{11}\} N \, d\Omega$$

$$K_M = \int_{\Omega} \frac{\partial N^T}{\partial x_k} \{\Delta D_v\} \frac{\partial N}{\partial x_k} \, d\Omega + \int_{\Gamma} N^T \{h_M\} N \, d\Gamma$$

$$K_{MT} = \int_{\Omega} \frac{\partial N^T}{\partial x_k} \{F_{12} k_e\} \frac{\partial N}{\partial x_k} \, d\Omega + \int_{\Gamma} N^T \{F_{12} h_T\} N \, d\Gamma +$$

$$\int_{\Gamma} N^T (Na_T)^3 \left\{ F_{12} \sigma \left(\epsilon + \sum_{j=1}^{nos} F_{i-j} \right) \right\} N \, d\Gamma$$

$$F_M = \int_{\Gamma} N^T \left\{ h_M q_{v,\alpha} + q''_M + F_{12} (h_T T_\alpha + q''_T + \sigma \epsilon T s^4 + \sigma \sum_{j=1}^{nos} F_{i-j} T_j^4) \right\} d\Gamma$$

The capacitance, stiffness matrices and the force vectors defined above are applicable for one-, two- and three-dimensional simulations. Additionally, mixed

dimensional problems can also be simulated. In other words, a certain part of the problem can be simulated in 3-D and a certain part of the problem can be simulated in 1-D. For one-dimensional problems, $d\Omega$ and $d\Gamma$ must be replaced by $A dL$ and A , where A is the cross section of the element and L is the element length. For two-dimensional problems, $d\Omega$ and $d\Gamma$ must be replaced by $t dA$ and $t dL$, where t is the thickness of the element. For three-dimensional problems, $d\Omega$ and $d\Gamma$ must be replaced by dV and dA , where V is the volume of the element. Equations (29) and (30) can be solved with various time integration schemes. The different time integration schemes can be written in the following format:

$$\begin{vmatrix} C_T + K_T \theta \Delta \tau & K_{TM} \theta \Delta \tau \\ K_{MT} \theta \Delta \tau & C_M + K_M \theta \Delta \tau \end{vmatrix} \begin{vmatrix} a_T^{r+\Delta \tau} \\ a_\rho^{r+\Delta \tau} \end{vmatrix} = \begin{vmatrix} [C_T - K_T(1-\theta)\Delta \tau] a_T^r \\ [C_M - K_M(1-\theta)\Delta \tau] a_\rho^r \end{vmatrix} - \begin{vmatrix} K_{TM}(1-\theta)\Delta \tau & a_\rho^r \\ K_{MT}(1-\theta)\Delta \tau & a_T^r \end{vmatrix} + \begin{vmatrix} F_T^r(1-\theta)\Delta \tau \\ F_M^r(1-\theta)\Delta \tau \end{vmatrix} + \begin{vmatrix} F_T^{r+\Delta \tau} \theta \Delta \tau \\ F_M^{r+\Delta \tau} \theta \Delta \tau \end{vmatrix} \quad (31)$$

The parameter θ used in Eq. (31) depends on the type of integration scheme. θ takes on values 0, 1/2 and 1 for the forward, central, and backward difference schemes, respectively.

SOLUTION PROCEDURE

Equations (27) and (28) give the room temperature and humidity ratio, respectively. However, these equations require knowing surface temperature and water vapor density, which are calculated from Eq. (31). But Eq. (31) requires knowing the "zone" conditions. Consequently, Eqs. (27), (28) and (31) must be solved simultaneously.

These equations can be solved with different methods: fixed point iteration, Newton type methods, and incremental methods, to name a few. Ortega and Rheinboldt (1980) provides an excellent survey of available procedures. A

particularly simple scheme is a fixed point iteration procedure known as successive substitution (also referred to as Picard iteration, functional iteration, and successive approximation). In this scheme the rate of convergence can be enhanced by using a relaxation factor. An outline of the fixed point iteration scheme is provided in Table 1.

The dependence of material properties on the field variables, and especially of the properties derived from the sorption curve, makes the problem highly nonlinear. Thus, fixed point iteration may not be the best solution method. The computer program developed uses fixed point and Newton Raphson iteration schemes. Several test cases have been executed and convergence has been achieved with both schemes. The Newton Raphson method converged much faster for each case but requires calculation of the Jacobian matrix. However, the definition and the construction of the Jacobian matrix is beyond the scope of this paper and is not given here.

RESULTS

For a linear sorption curve and a set of linear material properties the analytical solutions of Eqs. (18) and (19) for various boundary conditions are given by Dabir (1988) and Razzaq (1988). In this paper, validations pertaining to convective boundary conditions are presented. The temperature and water vapor density histories of a 10 cm thick infinite plate are depicted in Figures 2 and 3, respectively. One end ($X=0$) of the plate is assumed to be insulated and impermeable whereas the other end ($X=L$) is assumed to be exposed to convective boundary conditions. The sketch of the physical problem, material properties, sorption curve, simulation parameters, and initial and boundary conditions are given in the figures. This simulation uses consistent capacitance matrix and time step of 0.25 hour.

The following three example simulations illustrate the physics and the concept of "evaporation and condensation" theory. The material properties used in the simulations are for gypsum drywall and are represented in Table 2. Sketches of the physical problem are shown in appropriate figures. All the properties (except the tortuosity) are assumed to be nonlinear and varying, according to the equations given earlier.

Example 1: A 10 cm thick gypsum drywall sample is assumed to be insulated and impermeable at one end ($X=0$), and impermeable and exposed to convective heat transfer boundary conditions at the other end ($X=L$). In other words, heat is allowed to cross the sample at only $X=L$. However, moisture is not allowed to cross any boundary and the total mass of moisture is always preserved. The initial temperature and water vapor density are assumed to be $26.85\text{ }^{\circ}\text{C}$ and 0.012 kg/m^3 , respectively. The convective heat transfer coefficient and the temperature are $5.0\text{ W/m}^2\cdot^{\circ}\text{C}$ and $36.85\text{ }^{\circ}\text{C}$, respectively.

Figure 4.(a) shows the temperature distribution in the drywall sample. At the beginning, the temperature of the surface is hotter than the inner regions. Consequently, near the surface liquid water is converted into vapor, resulting in lower liquid water densities as shown in Figure 4.(d), and higher vapor densities as shown in Figure 4.(b). As the partial vapor pressure of the surface increases, a pressure gradient is created between the surface and inner regions of the sample, as shown in Figure 4.(c). Thus, the moisture is transported to the inner regions, resulting in higher liquid water densities. As the steady-state condition is reached, the moisture content levels off and attains its initial value (0.048 kg/kg) throughout the sample.

Example 2: A 10 cm thick gypsum drywall sample is assumed to be insulated and impermeable at one end ($X=0$), and insulated and exposed to convective mass

transfer boundary conditions at the other end ($X=L$). In other words, moisture is allowed to cross the sample at only $X=L$. However, heat is not allowed to cross any boundary. The initial temperature and water vapor density are assumed to be $26.85\text{ }^{\circ}\text{C}$ and 0.012 kg/m^3 , respectively. The convective mass transfer coefficient and the water vapor density are 0.005 m/s and 0.015 kg/m^3 , respectively.

Figures 5.(b) and 5.(c) show the water vapor density and partial vapor pressure distribution in the drywall sample. The vapor density and the partial vapor pressure of the surface reach the ambient value very rapidly, resulting in sharp increase in the liquid water content of the surface, as shown in Figure 5.(d). However, as the steady-state condition is reached, the moisture is slowly diffused to the inner regions of the sample. While the moisture is adsorbed, due to the heat of sorption, the temperature of the plate is increased, as shown in Figure 5.(d). However, due to the high thermal conductivity of the sample, except at the beginning, no appreciable temperature gradients are observed.

Example 3: A 1.27 cm thick gypsum drywall sample is assumed to be insulated and impermeable at one end ($X=0$), and exposed to convective heat and mass transfer boundary conditions at the other end ($X=L$). The initial temperature and water vapor density are assumed to be $26.85\text{ }^{\circ}\text{C}$ and 0.013 kg/m^3 , respectively. The convective heat transfer coefficient and the temperature are $5.0\text{ W/m}^2\cdot^{\circ}\text{C}$ and $22.85\text{ }^{\circ}\text{C}$, respectively. The convective mass transfer coefficient and the water vapor density are 0.005 m/s and 0.018 kg/m^3 , respectively. The initial and final conditions translate into relative humidities of 50.95 and 88.37 percent. Figure 6.(a) shows the temperature decay. Increase in the water vapor density and liquid water density are depicted in Figures 6.(b) and 6.(d), respectively.

CONCLUSIONS

Solutions to the equations give the detailed behavior of combined heat and moisture transfer in hygroscopic materials. However, the "evaporation and condensation" theory must be verified with experiments because different types of materials have different characteristics. The sorption curve derivatives used in the transport coefficients need to be experimentally verified. Experimental transport coefficient data, as a function of temperature and moisture content, are required. However, very little data pertaining to building materials can be found in the world literature.

ACKNOWLEDGEMENTS

The work reported here is funded under GRI contract #5087-243-1515 with the Gas Research Institute, 860 West Bryn Mawr Ave., Chicago, Illinois, and DOE cooperative agreement #DE-FC03-865F16305 with the Department of Energy San Francisco Operations Office, 1333 Broadway, Oakland, California. The authors thank Doug Kosar of GRI and David Pellish of DOE-Solar for their continued support of this research. The authors also thank Philip Fairey and Subrato Chandra for helpful discussions.

NOMENCLATURE

A	Heat and moisture transfer surface area [m^2]
A_T	Isothermal moisture capacity based on water vapor density [m^3/kg]
a_T	Nodal temperature unknown vector [K]
a	Nodal water vapor density unknown vector [kg/m^3]
B^p	Thermo-gradient coefficient based on water vapor density [$kg/kg.K$]
C_p^p	Specific heat [$J/kg.K$]
D_a^p	Molecular diffusivity of water vapor in air [m^2/s]
D_v	Moisture diffusivity [m^2/s]
h_{M_x}	Convective mass transfer coefficient [m/s]
h_M	Convective mass transfer coefficient (h_{M_a}) [$kg/m^2.s$]
h_T	Convective heat transfer coefficient [$W/m^2.K$]
i	Summation index over surface number one
J_v	Water vapor flux [$kg/m^2.s$]
k	Thermal conductivity [$W/m.K$]
L	Length [m]
m	Mass flow rate of the infiltration air [kg/s]

N	Shape function vector
nos	Number of surfaces
P	Total pressure [Pa]
P_v	Partial water vapor pressure [Pa]
Q_M	Moisture generation rate [kg/s]
$Q_{M,W}$	Moisture adsorbed or desorbed by the solid domain [kg/s]
Q_T	Heat generation rate [W]
q_T	Imposed heat flux [W/m^2]
$Q_{T,W}$	Heat taken or released by the solid domain [W]
R_v	Ideal gas constant [461.52 J/kg.K]
T	Temperature [K]
T_j	Temperature of the other surface [K]
T_r	Dry-bulb temperature of the "zone" air [K]
$T_{r,0}$	Initial "zone" air temperature [K]
T_s	Radiation receiver temperature [K]
U	Moisture content [kg/kg]
V	Volume [m^3]
W	Humidity ratio [kg/kg]
W_r	Humidity ratio of the "zone" air [kg/kg]
$W_{r,0}$	Initial "zone" air humidity ratio [kg/kg]
Γ_a	Interior envelope surface
Γ_e	Exterior envelope surface
Γ_f	Exterior furniture surface
ϵ	Emissivity or error tolerance
θ	Numerical integration constant [$0 \leq \theta \leq 1$]
Δ	Porosity
λ	Heat of vaporization [J/kg]
π	Permeability [s]
π_m	Permeance [h/s]
ρ	Density [kg/m^3]
σ	Stefan-Boltzmann constant [$W/m^2.K^4$]
τ	Time [s]
τ_0	Tortuosity
ϕ	Relative humidity [0 to 1]
Ω_a	Air domain
Ω_e	Envelope domain
Ω_f	Furniture and internal mass domain

SUBSCRIPTS AND SUPERSSCRIPTS

a	Air
b	Bulk
e	Effective or equilibrium
s	Solid
sat	Saturation
v	Vapor
α	Ambient
*	Surface condition

REFERENCES

- Berger, D.; and Pei, D.C.T. 1973. "Drying of Hygroscopic Capillary Porous Solids - A Theoretical Approach." Int. J. Heat Mass Transfer, Vol. 16, pp. 293-302.
- Cary, J.W.; and Taylor, S.A. 1962. "The Interaction of Simultaneous Diffusion of Heat and Water Vapor." Soil Sci., Am. Proc., Vol. 28, pp. 167-172.
- Crank, J. 1964. The Mathematics of Diffusion, Amen House London: Oxford University Press.
- Dabir, R. 1988. "Finite Element Analysis of Heat-Mass and Momentum Transfer in Hygroscopic Duct Systems." M.S. Thesis, Florida Institute of Technology.
- DeVries, D.A. 1958. "Simultaneous Transfer of Heat and Moisture in Porous Media." Trans. Am. Geophys. Union, Vol. 39, No. 5, pp. 909-916.
- DeVries, D.A. 1987. "The Theory of Heat and Moisture Transfer in Porous Media Revisited." Int. J. Heat Mass Transfer, Vol. 30, No. 7, pp. 1343-1350.
- Fitts, D.D. 1962. Non-Equilibrium Thermodynamics, New York: McGraw-Hill.
- Fortes, M.; and Okos, M.R. 1978. "A Non-Equilibrium Thermodynamics Approach to Transport Phenomena in Capillary Porous Media." Proceedings of the First International Symposium on Drying, McGill University, Montreal, pp. 100-109.
- Fortes, M.; and Okos, M.R. 1980. "Drying Theories: Their Bases and Limitations as Applied to Food and Grains." in Advances in Drying, Vol. 1, Edited by Mujumdar, A.S., New York: Hemisphere Publishing Co.
- Groot, S.R. 1951. Thermodynamics of Irreversible Processes, 2d. Ed., New York: Wiley.
- Groot, S.R. 1961. "On the Thermodynamics of Irreversible Heat and Mass Transfer." Int. J. Heat Mass Transfer, Vol. 4, pp. 63-70.
- Groot, S.R.; and Mazur, P. 1962. Non-Equilibrium Thermodynamics, Amsterdam: North Holland.
- Harmathy, T.Z. 1969. "Simultaneous Moisture and Heat Transfer in Porous Systems with Particular Reference to Drying." Ind. Chem. Fundam., Vol. 8, No. 1, pp. 92-103.
- Kerestecioglu, A.; Kamel, A; and Swami, M. 1988.a. "Theoretical and Computational Investigation of Simultaneous Heat and Moisture Transfer in Buildings: Effective Penetration Depth Theory." technical paper to be presented at the ASHRAE 1990 Winter Meeting and to be published in 1990 ASHRAE Transactions.
- Kerestecioglu, A.; Swami, M.; Dabir, R.; Razzaq, N.; and Fairey, P. 1988.b. "Theoretical and Computational Investigation of Algorithms for Simultaneous Heat and Moisture Transport in Buildings." final report to U.S. DOE contract #DE-FC03-865F16305 and GRI contract #5087-243-1515, FSEC-CR-191-88.
- Luikov, A.V. 1964. "Heat and Mass Transfer in Capillary Porous Bodies." in Advances in Heat Transfer, Irvine T.F. et al. (Eds)., Vol. 1, New York: Academic

Press.

Luikov A.V. 1966. Heat and Mass Transfer in Capillary-Porous Bodies, Oxford: Pergamon Press.

Luikov, A.V. 1975. "Systems of Differential Equations of Heat and Mass Transfer in Capillary-Porous Bodies (review)." Int. J. Heat Mass Transfer, Vol. 18., pp 1-14, 1975.

Ortega, J.M.; and Rheinboldt, W.C. 1980. Iterative Solution of Nonlinear Equations in Several Variables, New York: Academic Press.

Philip, J.R.; and DeVries, D.R. 1957. "Moisture Movement in Porous Media Under Temperature Gradients." Trans. Am. Geophysical Union, Vol. 38, No. 2, pp. 222-232.

Pierce, D.A.; and Benner, S.M. 1986. "Thermally Induced Hygroscopic Mass Transfer in a Fibrous Medium." Int. J. Heat Mass Transfer, Vol. 29, No. 11, pp. 1683-1694.

Prigogine, I. 1961. Introduction to Thermodynamics of Irreversible Processes, New York: Interscience Pub., Wiley.

Razzaq, N. 1988. "Finite Element Analysis of Enthalpy Storage Duct Systems." M.S. Thesis, Florida Institute of Technology.

Roques, M.A.; and Cornish, A.R.H. 1980. "Phenomenological Coefficients for Heat and Mass Transfer Equations in Wet Porous Media." in Drying'80, Vol. 2, Edited by Mujumdar, A.S., New York: Hemisphere Publishing Co.

Sherwood, T.K.; and Pigford, R.L. 1952. Absorption and Extraction, New York: McGraw-Hill Book Co.

Taylor, S.A.; and Cary, J.W. 1964. "Linear Equations for the Simultaneous Flow Matter and Energy in Continuous Soil System." Soil Sci., Soc. Am. Proc., Vol. 28, pp. 167-172.

Tveit, A. 1966. "Measurement of Moisture Sorption and Permeability of Porous Materials." Norwegian Building Research Institute Report No. 45, Oslo.

Valchar, J. 1966. "Heat and Moisture Transfer in Capillary Porous Materials from the Point of View of the Thermodynamics of Irreversible Processes." Third Int., Heat Transfer Conference, Chicago, Vol. 1, pp. 409-418.

TABLE 1
Fixed Point Iteration Scheme

- <1> Solve Eq. (31) with $T_{r,o}$ and $W_{r,o}$. Obtain $a_T(n, r+\Delta\tau)$ and $a_\rho(n, r+\Delta\tau)$
- <2> With known T^* and ρ_v^* solve Eqs. (27) and (28) to obtain T_r and W_r .
- <3> Check for convergence
- $$|a_T(n+1, r+\Delta\tau) - a_T(n, r+\Delta\tau)| < \epsilon \quad |T_r(n+1) - T_r(n)| < \epsilon$$
- $$|a_\rho(n+1, r+\Delta\tau) - a_\rho(n, r+\Delta\tau)| < \epsilon \quad |W_r(n+1) - W_r(n)| < \epsilon$$
- <4> If the solution converges increment the time and go to step <1>
- <5> If the solution does not converge, relax the solution using the following equations:
- $$a_T(n+1, r+\Delta\tau) = \mathfrak{R} a_T(n+1, r+\Delta\tau) + (1-\mathfrak{R}) a_T(n, r+\Delta\tau)$$
- $$a_\rho(n+1, r+\Delta\tau) = \mathfrak{R} a_\rho(n+1, r+\Delta\tau) + (1-\mathfrak{R}) a_\rho(n, r+\Delta\tau)$$
- $$T_r(n+1) = \mathfrak{R} T_r(n+1) + (1-\mathfrak{R}) T_r(n)$$
- $$W_r(n+1) = \mathfrak{R} W_r(n+1) + (1-\mathfrak{R}) W_r(n)$$
- <6> Let $T_{r,o} = T_r(n+1)$ and $W_{r,o} = W_r(n+1)$. Go to step <1>.

Note: n denotes the iteration number, ϵ denotes the error tolerance, and \mathfrak{R} is the relaxation parameter.

TABLE 2
Material Properties of Gypsum Drywall

k	ρ	C_p	τ_0	Λ_s	a	b	c	d
W/m.K	kg/m ³	J/kg.K						
0.262	725	1085	6	0.7	0.0107	8.8018	0.0615	0.3311

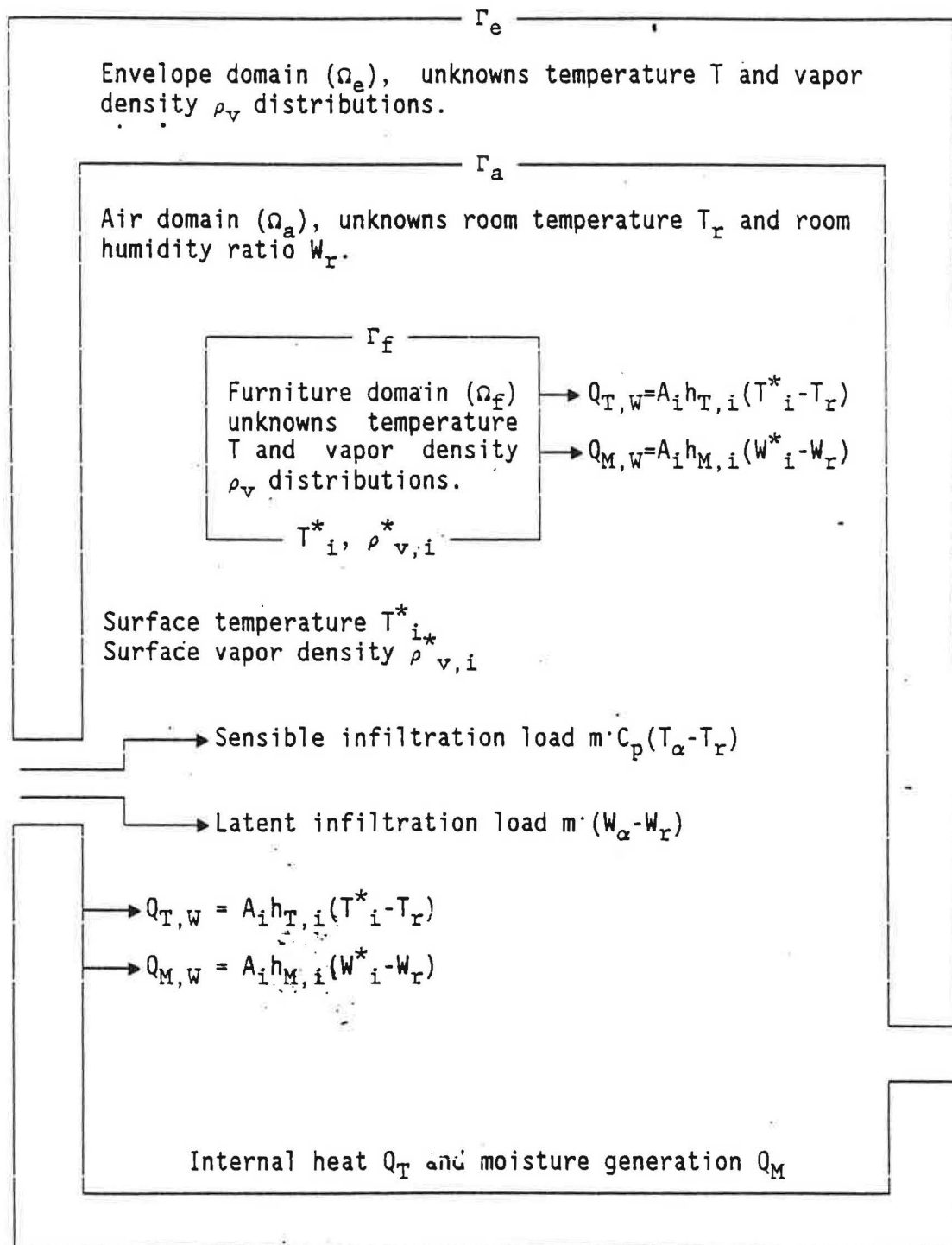


Figure 1. Schematic of the problem description and domain and surface definitions.

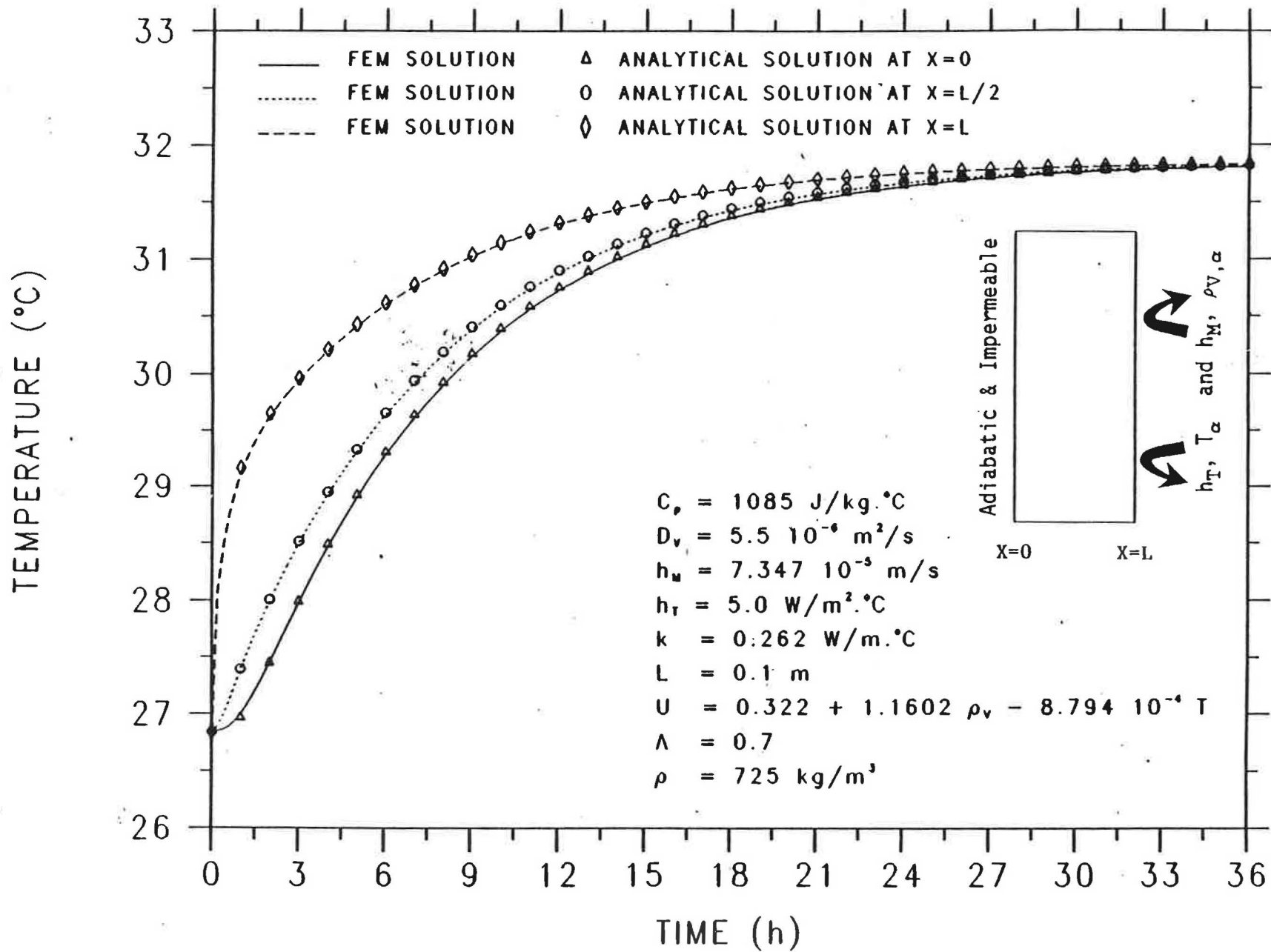


Figure 2. Comparison of analytical versus finite element temperature distribution in a gypsum drywall sample exposed to convective boundary conditions.

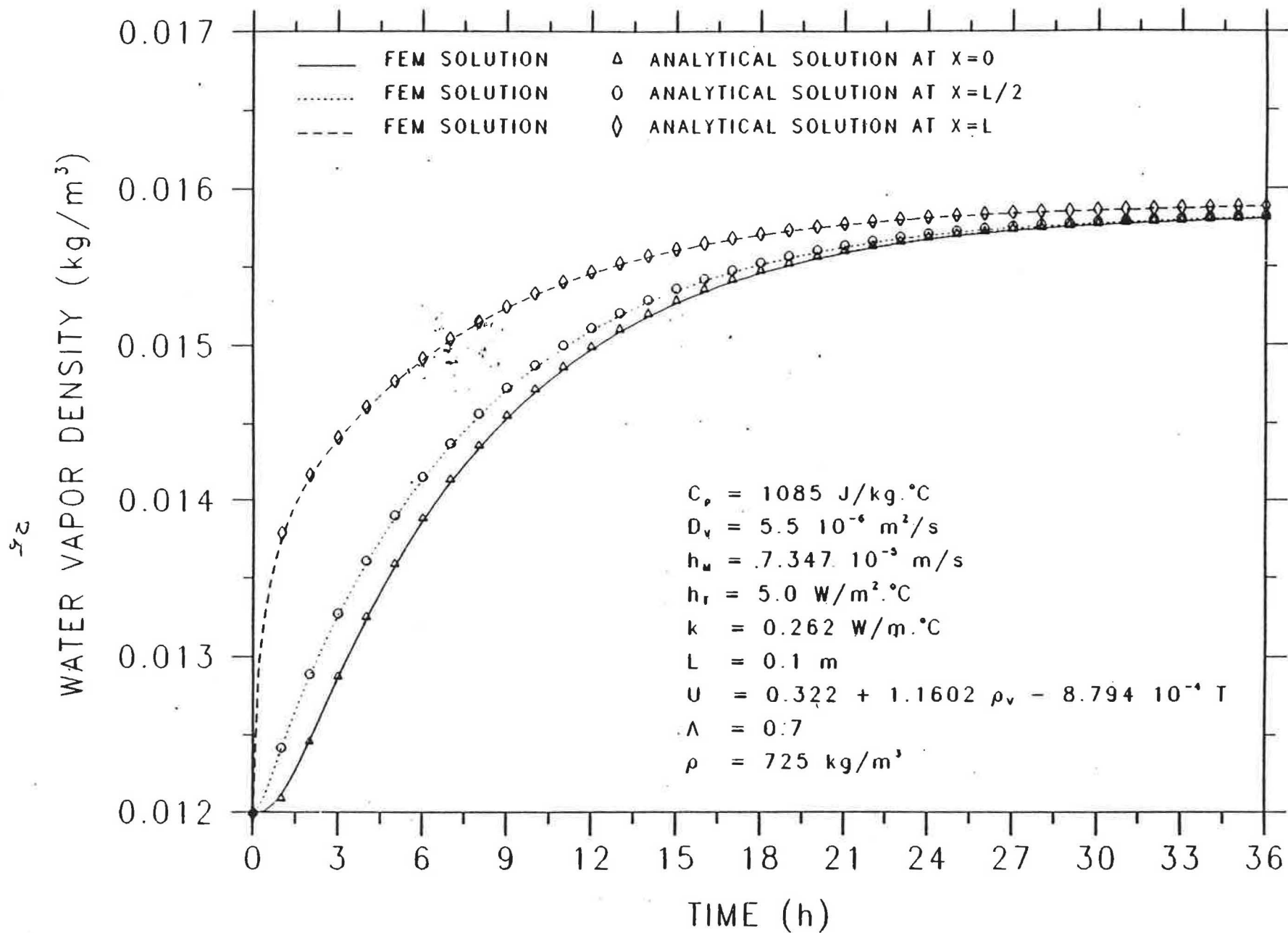


Figure 3. Comparison of analytical versus finite element water vapor density distribution in a gypsum drywall sample exposed to convective boundary conditions.

26

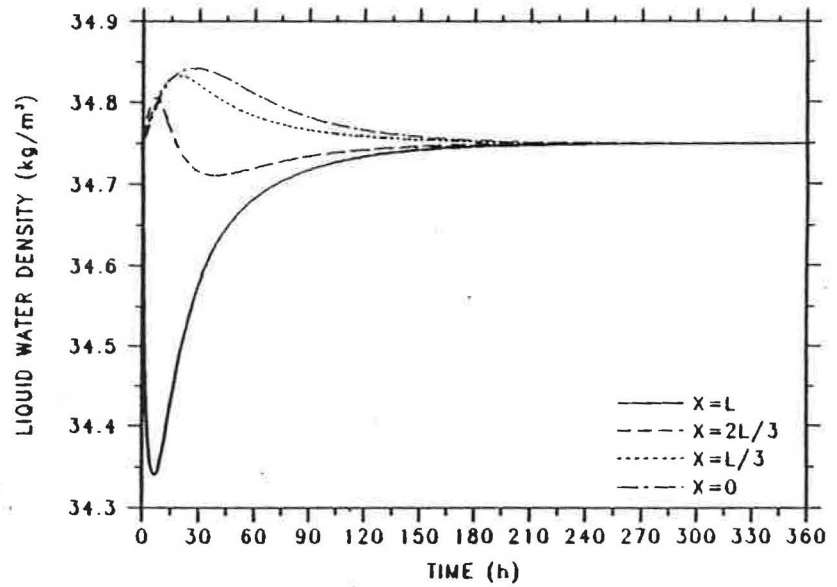
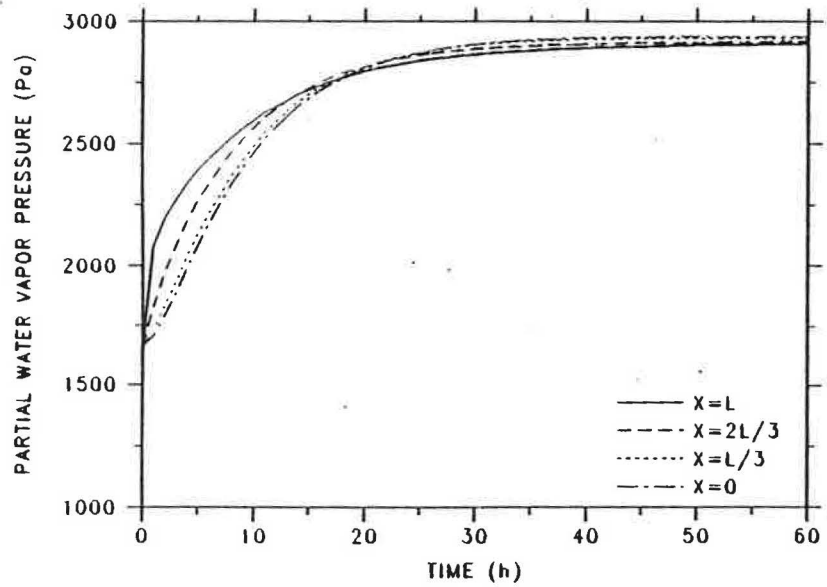
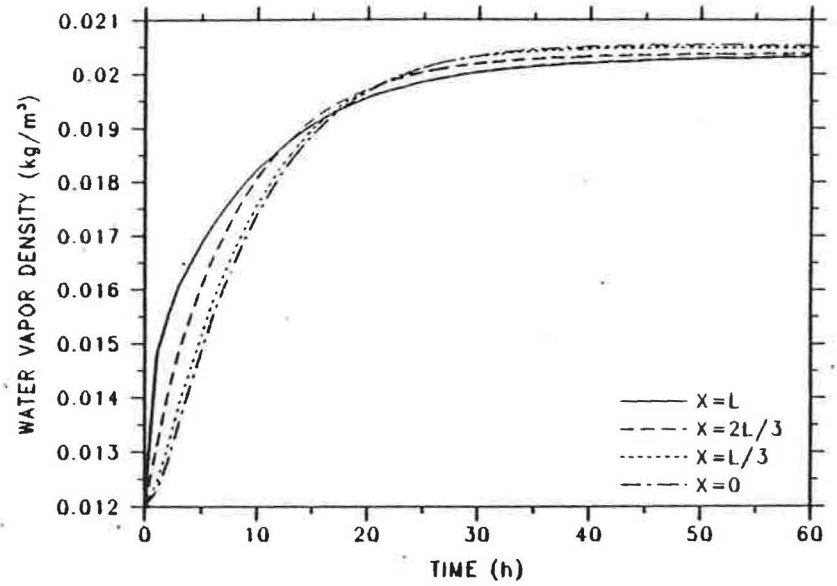
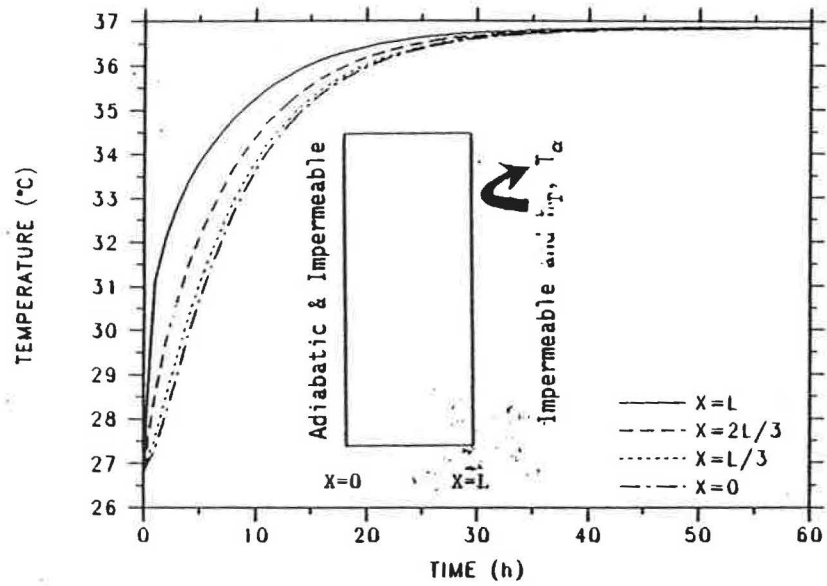


Figure 4. Redistribution of liquid and vapor in gypsum drywall resulting from a change in temperature at the impermeable convective boundary.

27

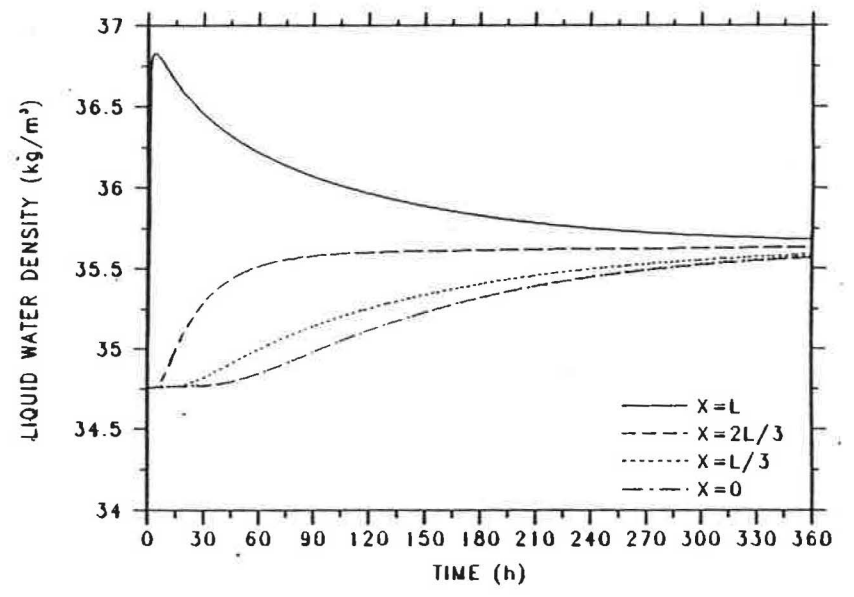
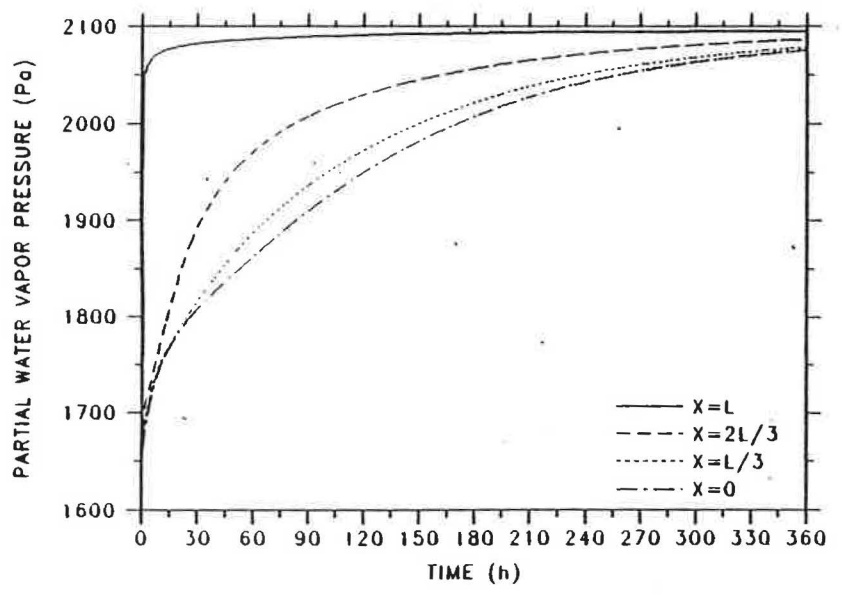
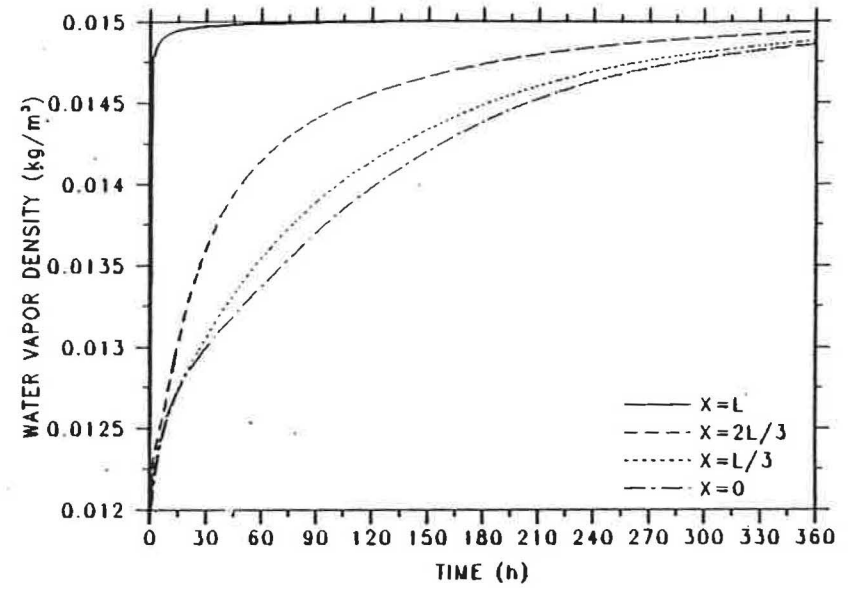
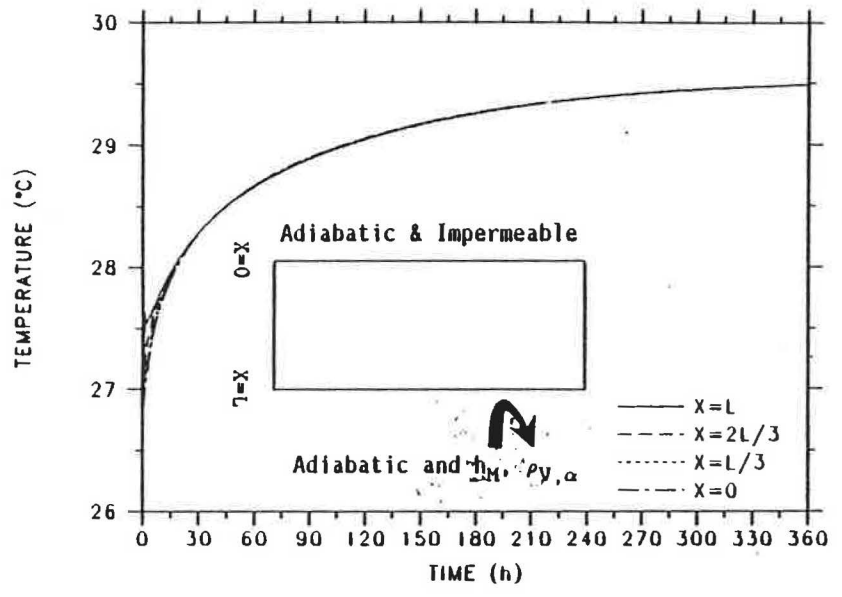


Figure 5. Redistribution of liquid and vapor in gypsum drywall resulting from a change in vapor density at the adiabatic convective boundary.

82

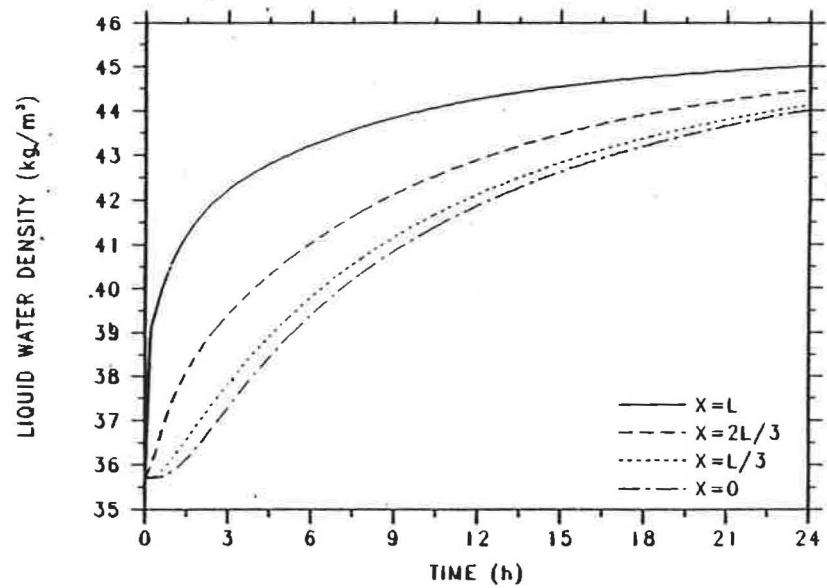
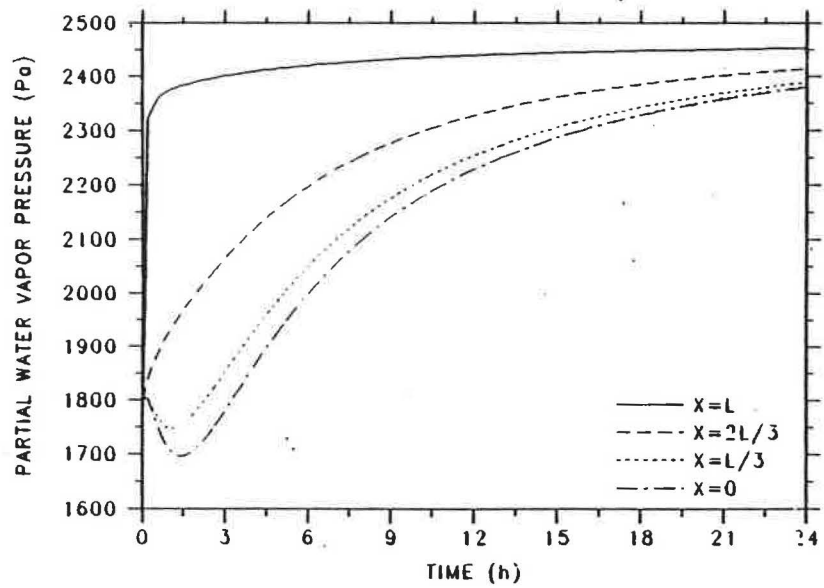
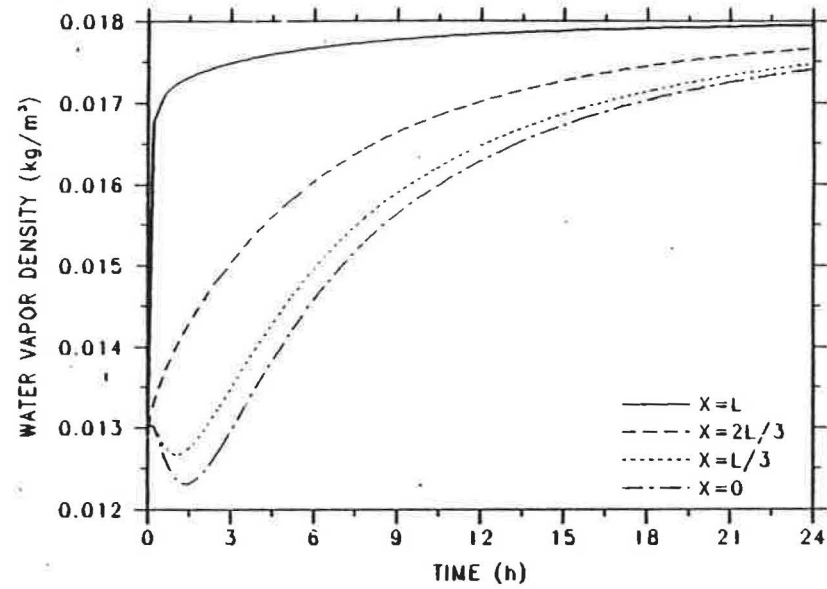
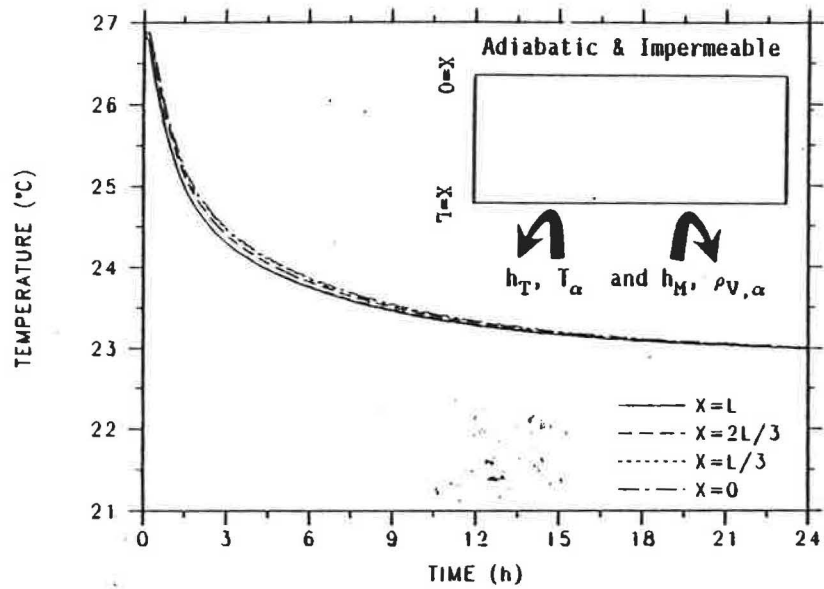


Figure 6. Temperature and moisture history in gypsum drywall resulting from a change in temperature and vapor density at the convective boundary.